

## Garnet-type $\text{Li}_7\text{La}_3\text{Zr}_2\text{O}_{12}$ Electrolyte Prepared by a Solution-Based Technique for Lithium ion battery

Jiajia Tan<sup>1</sup> and Ashutosh Tiwari<sup>1</sup>

<sup>1</sup>Nanomaterials Research Laboratory, Department of Materials Science and Engineering, University of Utah, Salt Lake City, UT 84112, U.S.A.

### ABSTRACT

High quality garnet-type  $\text{Li}_7\text{La}_3\text{Zr}_2\text{O}_{12}$  solid electrolyte was synthesized using a solution-based technique. The electrolyte pellets were sintered at 900 °C, resulting in tetragonal phase, which then transformed to cubic phase after annealing at 1230 °C. The ionic conductivity of both phases was studied and revealed to be  $3.67 \times 10^{-7}$  S/cm and  $1.67 \times 10^{-4}$  S/cm, respectively. A prototype cell comprising of  $\text{Li}_7\text{La}_3\text{Zr}_2\text{O}_{12}$  electrolyte,  $\text{LiCoO}_2$  cathode and lithium metal anode was assembled. The cell made with the cubic phase electrolyte exhibited superior performance than the one made with the tetragonal phase electrolyte. The former cell possessed a very promising gravimetric discharge capacity of 3.4 mAh/g, which is the highest value obtained among similar setups.

### INTRODUCTION

Lithium ion batteries (LIBs) have attracted a lot of attention over recent decades and have become an essential part in many of our portable electronic devices. Recently, the field of LIBs is further stimulated by the development of novel electric automobiles, which depends on the achievement of reliable power sources. Such power suppliers should be able to deliver a high power in an extended period of time and be able to restore quickly; as well, they must be intrinsically safe, especially at high temperatures.

However, current LIBs couldn't satisfy those requirements very well, since they use liquid organic electrolytes, which are toxic, prone to leakage, and are highly flammable. To substitute the conventional organic liquids, various kinds of solid-state electrolytes have been investigated, mainly glass or glass ceramics consisting of oxides, sulphides or a mixture of both [1-4]. Unfortunately, they have either high ionic conductivity or good chemical stability, rather than having both. Lately, a garnet-type  $\text{Li}_7\text{La}_3\text{Zr}_2\text{O}_{12}$  (LLZO) electrolyte was synthesized by Weppner's group [5], which was a source of enthusiasm in the field of all-solid-state LIBs [6-8]. LLZO has practically high enough ionic conductivity, negligible electronic conductivity, and good chemical stability against possible electrode materials; in addition, it is environmentally benign, easy to fabricate and of low cost [9-10].

Till date, there have been many reports on synthesizing the LLZO electrolyte by solid-state method, which requires multiple grinding and sintering at high temperatures [8]. The method is not only energy and time consuming, but also can lead to severe lithium loss during multiple high temperature procedures. Here, we are reporting the synthesis of LLZO through a solution-based technique, where most of the processes were conducted at low temperatures. The structural features and electrical properties of LLZO are reported. Moreover, the electrochemical behavior of the LLZO pellet is described as an electrolyte in a  $\text{Li}/\text{LLZO}/\text{LiCoO}_2$  battery.

## EXPERIMENT

The experimental procedures for synthesizing LLZO are illustrated in Figure 1. Firstly, high purity powders of  $\text{ZrO}(\text{NO}_3)_2 \cdot 6\text{H}_2\text{O}$ ,  $\text{La}_2\text{O}_3$  and  $\text{Li}_2\text{CO}_3$  were dissolved in diluted nitric acid and mixed into one beaker with a molar ratio of 4: 3: 7.7. The extra 10% of  $\text{Li}_2\text{CO}_3$  was used to compensate the lithium loss by volatilization during sintering. After that, citric acid solution was added as the organic chelating agent. The PH value of the mixture was adjusted to 2 for achieving a transparent solution which was then transferred to a flask and refluxed for one hour. Next, the solution was concentrated and dried by evaporation on a hot plate. The dried powders were heated in air at 800 °C for 24 hrs. Lastly, the powders were ground and pressed into pellets (under 3500 psi) followed by calcinations at 900 °C or 1230 °C in air for 8 hrs (1 °C/min).

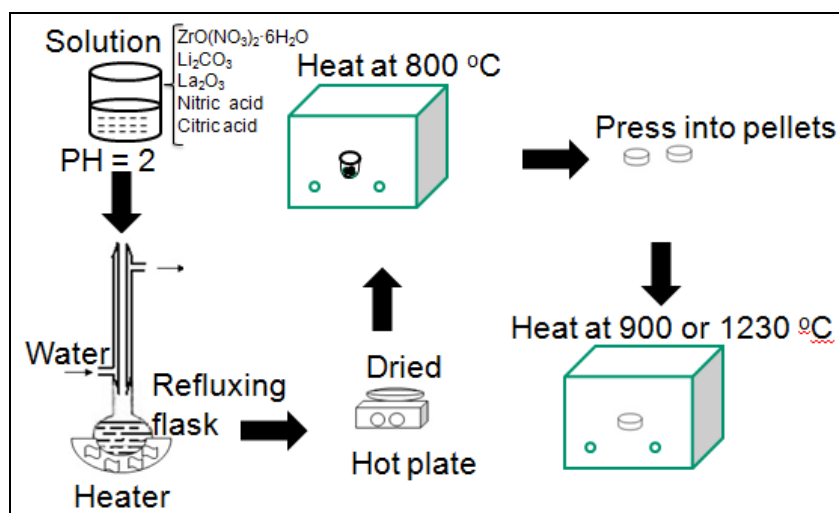


**Figure 1.** The schematic drawing of the experimental procedures.

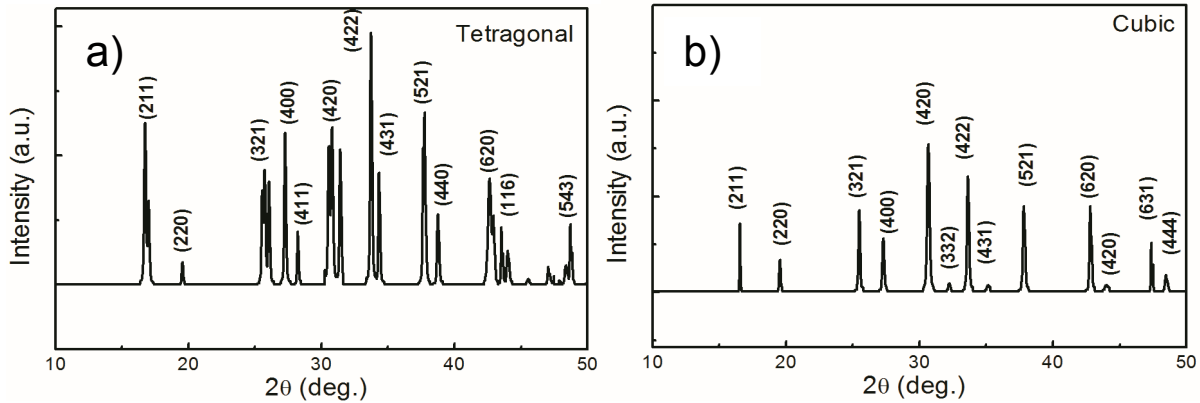
Crystal structure of the synthesized pellet was analyzed by X-ray powder diffraction (XRD) using  $\text{CuK}\alpha$  radiation with a wavelength of 1.54 Å. Surface morphology and chemical composition was characterized by scanning electron microscopy (SEM) and energy dispersive X-ray spectroscopy (EDS), respectively. The ionic conductivity of the sintered pellet (1.65 cm in diameter and 0.55 cm in thickness) was measured using the electrochemical impedance spectroscopy (EIS) function of a Gamry 600, in the frequency range of 1 MHz to 10 Hz. For this, gold was sputtered on the top and bottom surface of the LLZO pellets. Moreover, a proto-type Li/LLZO/  $\text{LiCoO}_2$  cell was made by simple tape-casting of  $\text{LiCoO}_2$  cathode slurry on one side of the LLZO pellet and then attaching a piece of lithium foil on the other side of the pellet. The detailed steps were described elsewhere [11]. Galvanostatic charge/discharge performance of the cells was recorded.

## DISCUSSION

### X-ray diffraction

Figure 2 shows the XRD patterns of the samples sintered at 900 °C and 1230 °C. As can be seen, the sample sintered at 900 °C is tetragonal, showing characteristic double peaks. The

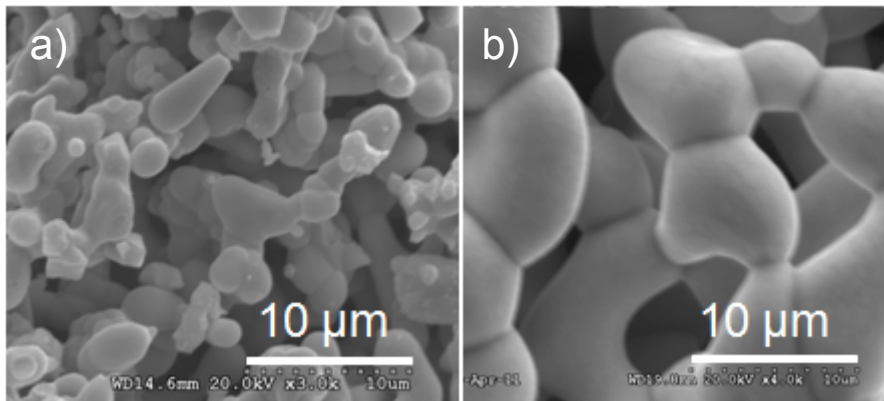
crystals belong to  $I4_1/acd$  space group, and the lattice constants were calculated to be  $a = 13.149 \text{ \AA}$ , and  $b = 12.698 \text{ \AA}$  ( $a = 13.134 \text{ \AA}$ ,  $b = 12.663 \text{ \AA}$ ) [6]. Whereas, the pellet sintered at  $1230 \text{ }^\circ\text{C}$  possessed cubic crystals, in the space group of  $Ia-3d$ . Using the Rietveld refinement, the lattice constant was found to be  $a = 12.8974 \text{ \AA}$  (similar to  $a = 12.9682 \text{ \AA}$  in the literature [12]). Although we obtained the tetragonal and cubic phase LLZO pellets by a solution based technique, the final sintering temperatures were similar to that required in solid state synthesis, but our method avoided repetitive heating and grinding steps, saving much time and energy.



**Figure 2.** XRD patterns of the LLZO pellets sintered at (a)  $900 \text{ }^\circ\text{C}$  and (b)  $1230 \text{ }^\circ\text{C}$ .

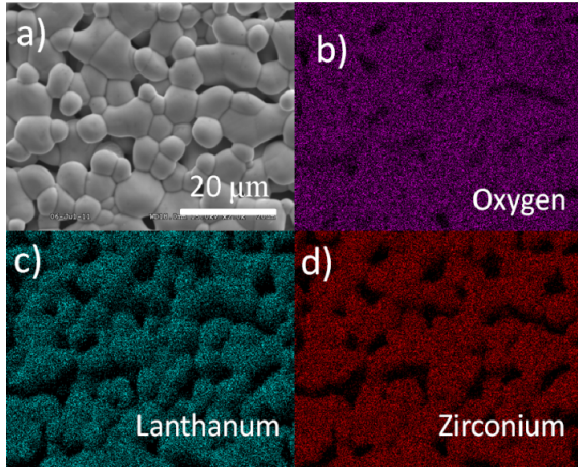
### Scanning electron microscopy

Figure 3a shows the SEM image of the LLZO material synthesized at  $900 \text{ }^\circ\text{C}$  for 8 hrs. As you see, the grains size is less than  $5 \mu\text{m}$  and the connection between grains are quite poor. Figure 3b shows the SEM image of the pellet sintered at  $1230 \text{ }^\circ\text{C}$ . The grains are larger at an average size of  $10 \mu\text{m}$ . Moreover, the grains contacted one another via grain boundaries, forming a continuous conduction path for lithium ions.



**Figure 3.** SEM images of the LLZO pellets sintered at (a)  $900 \text{ }^\circ\text{C}$  and (b)  $1230 \text{ }^\circ\text{C}$ .

EDS measurement was conducted on the LLZO sample sintered at  $1230 \text{ }^\circ\text{C}$ . The counts for oxygen, lanthanum and zirconium were found close to the stoichiometric atomic ratio. The elemental mapping for O, La and Zr is presented in Figure 4. These images clearly show that the three elements are distributed evenly throughout the surface, indicating the absence of phase separation or non-stoichiometric area.



**Figure 4.** Elemental mapping of oxygen, lanthanum and zirconium on LLZO pellet sintered at 1230 °C.

### Electrical properties

Figure 5 displays the room temperature Nyquist plots of the complex impedance for the tetragonal and cubic phase LLZO pellets, which were covered by ion-blocking Au electrodes. The curves could be regarded to consist of a compressed semicircle and a tail. The compressed semicircle at high frequencies could originate from the total electrical resistance through the bulk and grain boundaries. The tail at the low frequency range represents capacitive behavior between the ionic blocking gold electrodes, indicating the ionic nature of the LLZO pellet. The impedance data were fitted to an equivalent circuit model of  $(R_{tot}/Q_{tot})Q_{el}$  (solid line), where  $R_{tot}$  is the total resistance,  $Q$  is the constant phase element [13]. From the fitting results, the room temperature ionic conductivity was found to be  $3.67 \times 10^{-7}$  S/cm for the tetragonal phase LLZO, while the obtained value for cubic phase LLZO was  $1.67 \times 10^{-4}$  S/cm, almost three orders of magnitude higher than the former.

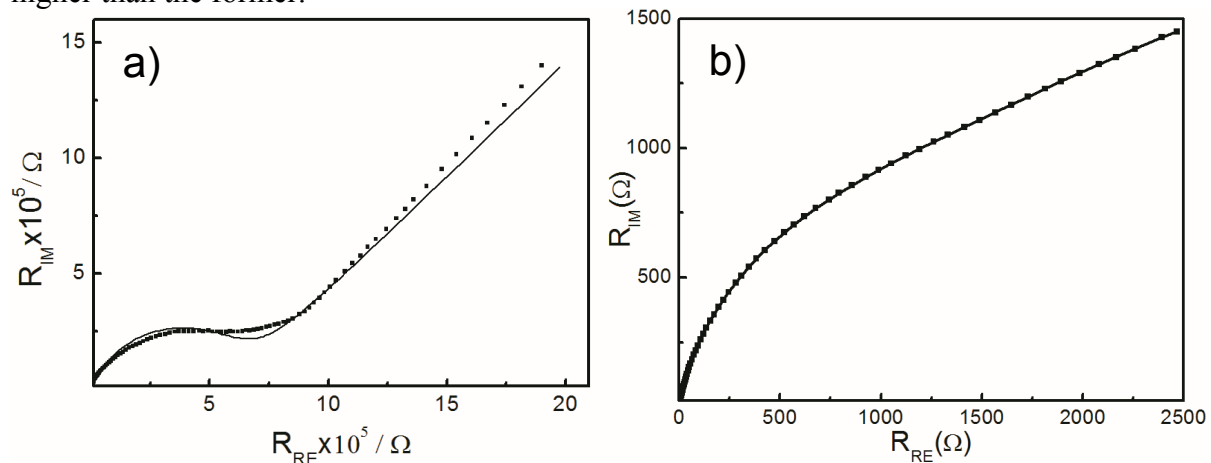


**Figure 5.** Nyquist impedance plots of the LLZO pellets sintered at (a) 900 °C and (b) 1230 °C.

In order to make an estimate of the activation energy, temperature dependent measurement of total ionic conductivity was performed over the range of room temperature to 100 °C (Figure 6). The ionic conductivities were found to fit well in the Arrhenius equation:

$$\sigma = (A/T)\exp(-E_a/(kT)) \quad (1)$$

where  $\sigma$  is the electrical conductivity,  $A$  is a constant,  $T$  is the absolute temperature,  $E_a$  is the activation energy and  $k$  is the Boltzmann's constant. Activation energy was calculated to be 0.61 eV and 0.36 eV for tetragonal and cubic LLZO, respectively.

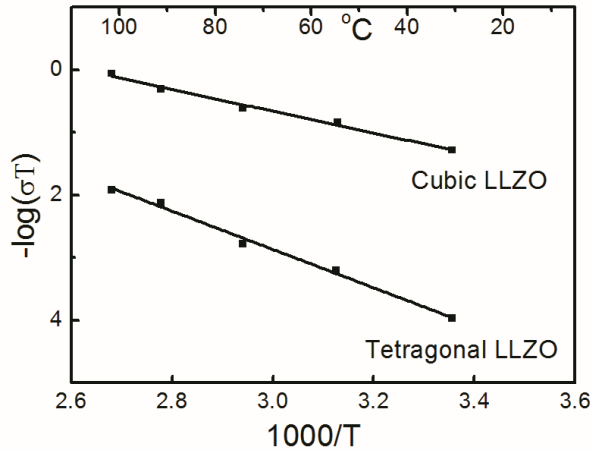


**Figure 6.** Arrhenius plot of the electrical properties for LLZO pellets.

### Charge/discharge behavior

Figure 7 shows the charge/discharge behavior of the all-solid-state Li/LLZO/LiCoO<sub>2</sub> cell, using cubic phase LLZO as the electrolyte. The specific discharge capacity of the cell, when cycled at 2  $\mu\text{A}/\text{cm}^2$ , was 20  $\mu\text{Ah}/\text{cm}^2$ , which was 3.4 mAh/g by taking the mass loading into account. The value is the highest among similar setups using tape-casted LiCoO<sub>2</sub> powders as the cathode. [6] Moreover, the capacity could be greatly increased by applying thin film techniques to fabricate LLZO/LiCoO<sub>2</sub> hetero-structure. Just a note, the cell using tetragonal LLZO as the electrolyte exhibited very little discharge capability less than 1 mAh/g, thus was not shown here.

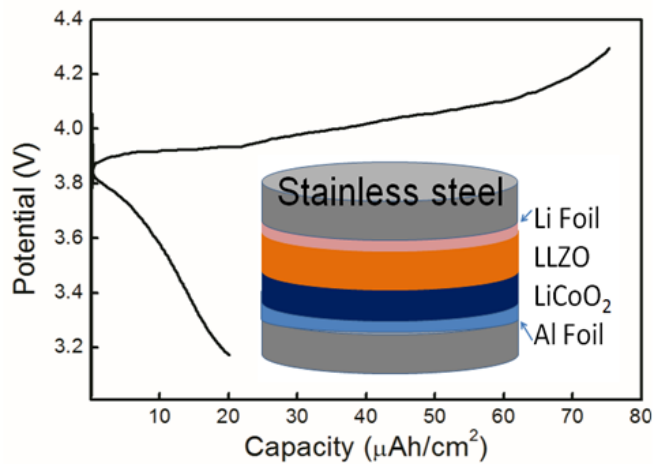


**Figure 7.** Charge/discharge curves and schematic drawing of the Li/LLZO/LiCoO<sub>2</sub> battery.

## CONCLUSIONS

We have successfully synthesized the LLZO solid electrolyte through a solution-based technique. The room temperature ionic conductivity of the tetragonal and cubic phase LLZO pellets was found to be  $3.67 \times 10^{-7}$  S/cm and  $1.67 \times 10^{-4}$  S/cm, respectively. The cubic phase LLZO electrolyte was assembled into a Li/LLZO/LiCoO<sub>2</sub> cell, displaying 3.4 mAh/g specific discharge capacity. We proved that the chemically stable LLZO electrolyte worked well when assembled in an all-solid-state cell with lithium metal and LiCoO<sub>2</sub>. Therefore, the cubic phase LLZO is a very promising solid electrolyte candidate for achieving safe and high power LIBs.

## REFERENCES

1. N. Ohta, K. Takada, L. Zhang, R. Ma, M. Osada, T. Sasaki, *Adv. Mater.* **18**, 2226 (2006).
2. T. Brousse, P. Fragnaud, R. Marchand, D.M. Schleich, O. Bohnke, K. West, *J. Power Sources* **68**, 412 (1997).
3. N. J. Dudney, B. J. Neudecker, *Curr. Opin. Solid State Mater. Sci.* **4**, 479 (1997).
4. M. Tatsumisago, F. Mizuno, A. Hayashi, *J. Power Sources* **159**, 193 (2006).
5. R. Murugan, V. Thangadurai, W. Weppner, *Angew. Chem. Int. Ed.* **46**, 7778 (2007).
6. M. Kotobuki, H. Munakata, K. Kanamura, Y. Sato, T. Yoshida, *J. Electrochem. Soc.* **157**, A1076 (2010).
7. J. Awaka, N. Kijima, H. Hayakawa, J. Akimoto, *J. Solid State Chem.* **182**, 2046 (2009).
8. C. A. Geiger, E. Alekseev, B. Lazic, M. Fisch, T. Armbruster, R. Langner, M. Fechtelkord, N. Kim, T. Pettke, W. Weppner, *Inorg. Chem.* **50**, 1089 (2011).
9. J. Awaka, A. Takashima, K. Kataoka, N. Kijima, Y. Idemoto, J. Akimoto, *Chem. Lett.* **40**, 60 (2011).
10. K. H. Kim, Y. Iriyama, K. Yamamoto, S. Kumazaki, T. Asaka, K. Tanabe, C. A.J. Fisher, T. Hirayama, R. Murugan, Z. Ogumi, *J. Power Sources* **196**, 764 (2011).
11. J. Tan and A. Tiwari, *Electrochem. Solid-State Lett.* **15**, A37 (2012).
12. A. Kuhn, S. Narayanan, L. Spencer, G. Goward, V. Thangadurai and M. Wilkening, *Phys. Rev. B* **83**, 094302 (2011).
13. I. Kokal, M. Somer, P.H.L. Notten and H.T. Hintzen, *Solid State Ionics* **185**, 42 (2011).